

In the format provided by the authors and unedited.

# The infrared spectrum of protonated buckminsterfullerene $C_{60}H^+$

Julianna Palotás<sup>1</sup>, Jonathan Martens <sup>1</sup>, Giel Berden <sup>1</sup> and Jos Oomens <sup>1,2\*</sup>

---

<sup>1</sup>Radboud University, Institute for Molecules and Materials, FELIX Laboratory, Nijmegen, The Netherlands. <sup>2</sup>van 't Hoff Institute for Molecular Sciences, University of Amsterdam, Amsterdam, The Netherlands. \*e-mail: [j.oomens@science.ru.nl](mailto:j.oomens@science.ru.nl)

# The infrared spectrum of protonated buckminsterfullerene, $C_{60}H^+$

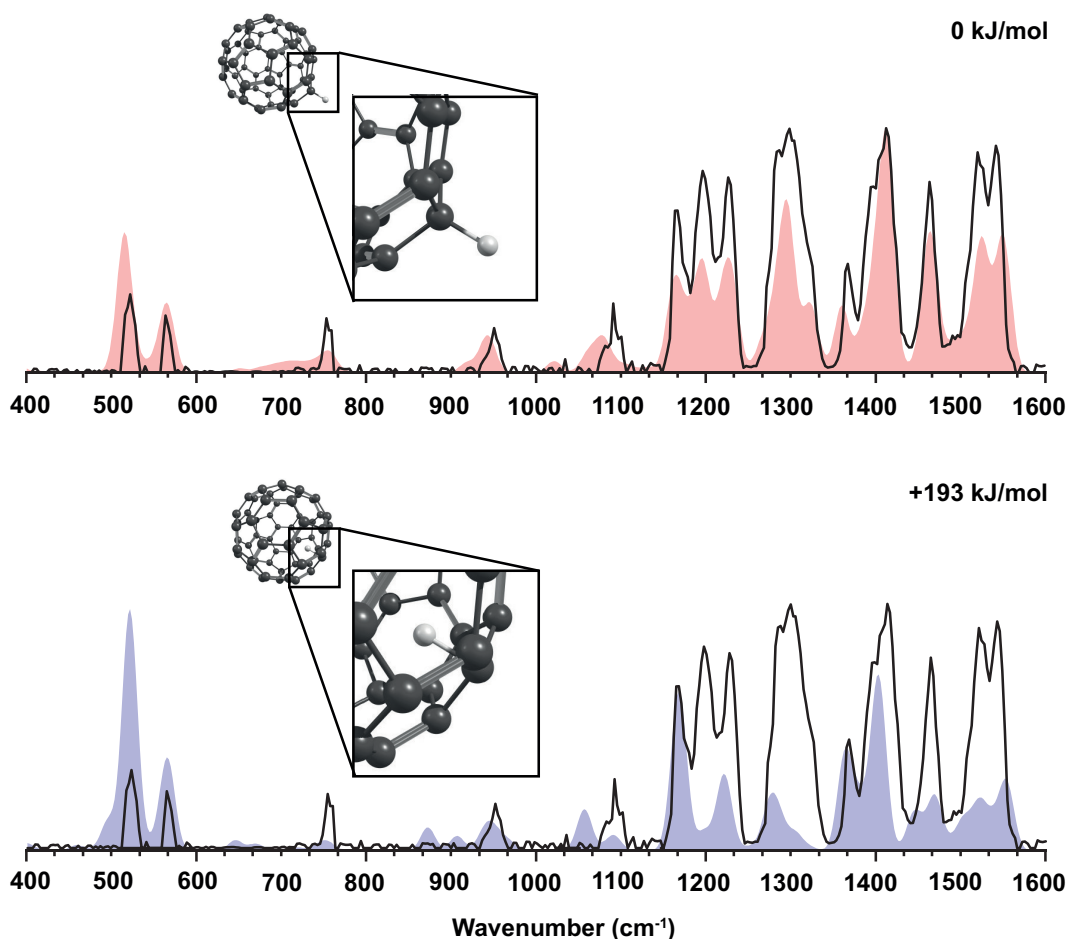
## Supplementary Information

Julianna Palotás,<sup>1</sup> Jonathan Martens,<sup>1</sup> Giel Berden,<sup>1</sup> and Jos Oomens<sup>1,2, a)</sup>

<sup>1</sup>*Radboud University, Institute for Molecules and Materials, FELIX Laboratory, Toernooiveld 7, 6525ED Nijmegen, The Netherlands*

<sup>2</sup>*van 't Hoff Institute for Molecular Sciences, University of Amsterdam, Science Park 908, 1098XH Amsterdam, The Netherlands*

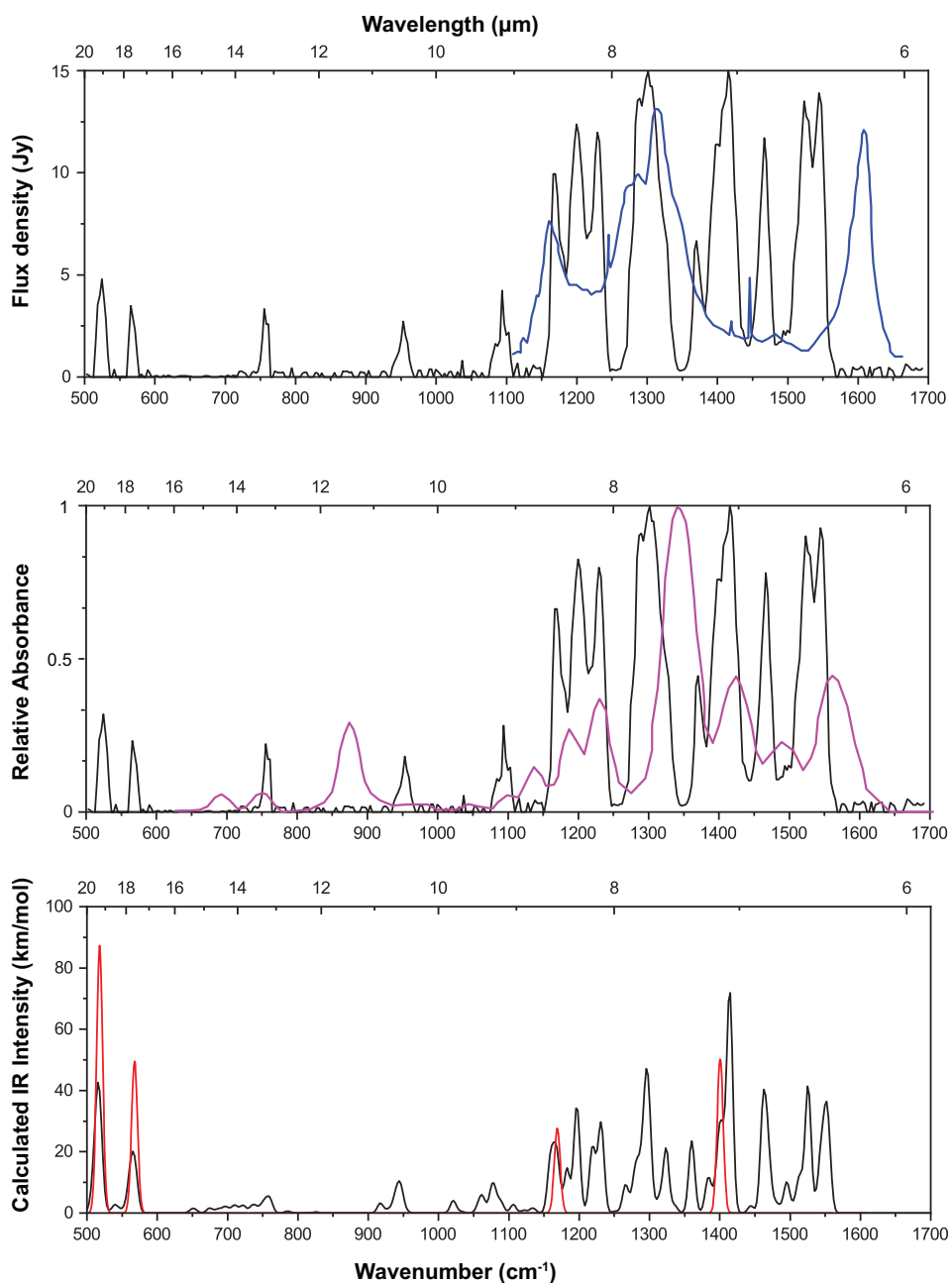
### ENDOHEDRAL VERSUS EXOHEDRAL PROTONATION



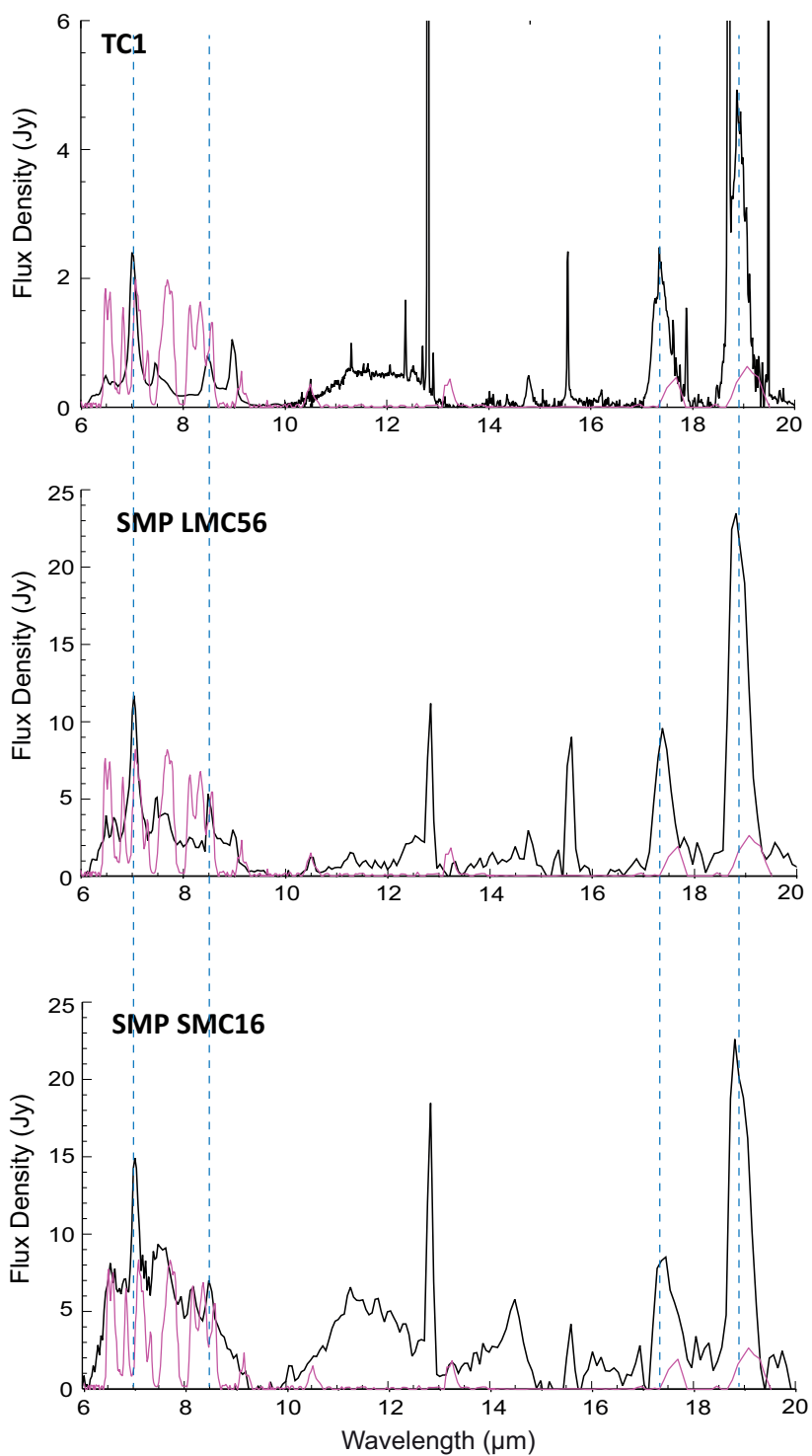
Supplementary Figure 1. Comparison of computed spectra (B3LYP/6-311+G(d,p)) for the two possible protonation sites: exohedral (top) or endohedral (bottom). Clearly, the experimental versus theoretical match is better for the exohedral structure. Relative Gibbs energies for the two structures, given in each panel in kJ/mol, also strongly favor the exohedral geometry.

<sup>a)</sup> Corresponding author: j.oomens@science.ru.nl

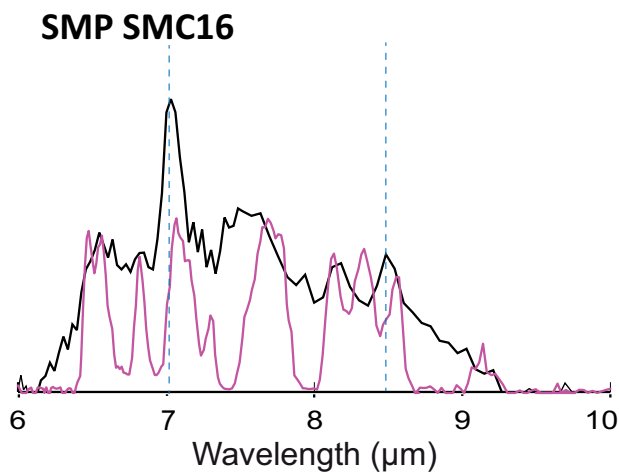
## SPECTRAL COMPARISONS



Supplementary Figure 2. **Top panel:** Comparison of the laboratory spectrum of C<sub>60</sub>H<sup>+</sup> (black) with an emission spectrum of NGC7023 obtained with the SWS spectrograph on board ISO (blue) with main features observed being attributed to PAHs.<sup>1</sup> **Middle panel:** Comparison with average theoretical spectrum of six cationic PAHs (anthracene, tetracene, 1,2-benzanthracene, chrysene, pyrene, and coronene).<sup>2</sup> Both spectra are clearly distinct from the C<sub>60</sub>H<sup>+</sup> spectrum. The bottom panel contrasts the theoretical spectra of C<sub>60</sub> (red) and C<sub>60</sub>H<sup>+</sup> (black).



Supplementary Figure 3. Comparison of the laboratory spectrum of  $\text{C}_{60}\text{H}^+$  with astronomical emission spectra observed from the planetary nebulae TC1, SMP SMC56, and SMP LMC16.<sup>3,4</sup> Dashed lines indicate band positions for neutral  $\text{C}_{60}$ .



Supplementary Figure 4. Detailed comparison of the laboratory spectrum of  $C_{60}H^+$  with Spitzer-IRS spectrum from the SMP SMC16 planetary nebula.<sup>3,4</sup> Dashed lines indicate band positions for neutral  $C_{60}$ .

#### CALCULATED IR SPECTRA AT DIFFERENT LEVELS OF DFT

Supplementary Table 1. Experimental band centers and band centers of the convoluted computed spectra (see Fig. 3 in the main text). The used scaling factor is shown for each computational method. The RMS deviation from the experimental band centers is given for each of the computational methods.

Method	IRMPD	B3LYP/ 3-21G (0.9650)	$\Delta$	B3LYP/ 4-31G (0.9752)	$\Delta$	BP86/ 4-31G (1.0033)	$\Delta$	B3LYP/ 6-311+G(p,d) (0.9679)	$\Delta$	M06-2X/ 6-311+G(p,d) (0.9520)	$\Delta$
Band center ( $cm^{-1}$ )	524	497.5	26.5	537.1	-13.1	522.5	1.5	515.5	8.5	510.2	13.8
	566	560.8	5.2	572.3	-6.3	572.9	-6.9	565.3	0.7	567.1	-1.1
	756	758.6	-2.6	768.4	-12.4	769.8	-13.8	754.7	1.3	757.8	-1.8
	953	943.6	9.4	957	-4	961.6	-8.6	944.1	8.9	938.7	14.3
	1094	1072.9	21.1	1092.8	1.2	1100.5	-6.5	1076.2	17.8	1065	29
	1167	1169.2	-2.2	1185.8	-18.8	1186.3	-19.3	1165.9	1.1	1166.5	0.5
	1199	1184.4	14.6	1211	-12	1206.5	-7.5	1195.8	3.2	1203.7	-4.7
	1229	1209.8	19.2	1238.6	-9.6	1236.8	-7.8	1225.7	3.3	1235.9	-6.9
	1301	1295.9	5.1	1319.1	-18.1	1322.6	-21.6	1295.4	5.6	1285.4	15.6
	1370	1356.8	13.2	1387	-17	1398.3	-28.3	1360.2	9.8	1369.6	0.4
	1415	1425.2	-10.2	1447.3	-32.3	1423	-8	1412.6	2.4	1424.1	-9.1
	1467	1470.8	-3.8	1495.1	-28.1	1499.3	-32.3	1464.9	2.1	1478.6	-11.6
	1523	1536.8	-13.8	1558	-35	1552.3	-29.3	1524.7	-1.7	1543.3	-20.3
	1545	1562.1	-17.1	1580.6	-35.6	1572.4	-27.4	1549.6	-4.6	1570.3	-25.3
	<b>RMSD</b>			3.68		5.49		4.96		1.83	

- **Supplementary Data 1:** The IRMPD spectrum of  $C_{60}H^+$  in ASCII format.
- **Supplementary Data 2:** Calculated IR spectrum for the exohedral  $C_{60}H^+$  geometry in ASCII format. Harmonic vibrational frequencies and intensities are calculated at the B3LYP/6-311+G(d,p) level of theory. No frequency scaling has been applied to these values.
- **Supplementary Data 3:** Calculated IR spectrum for the endohedral  $C_{60}H^+$  geometry in ASCII format. Harmonic vibrational frequencies and intensities are calculated at the B3LYP/6-311+G(d,p) level of theory. No frequency scaling has been applied to these values.
- **Supplementary Data 4:** Optimized geometry of  $C_{60}H^+$  (exohedral) at the B3LYP/6-311+G(d,p) level of theory.

## REFERENCES

- <sup>1</sup>Peeters, E. *et al.* The rich 6 to 9  $\mu\text{m}$  spectrum of interstellar PAHs. *Astron. Astrophys.* **390**, 1089-1113 (2002)
- <sup>2</sup>L. J. Allamandola, L. J., Hudgins, D. M. & Sandford, S. A. Modeling the unidentified infrared emission with combinations of polycyclic aromatic hydrocarbons. *Astrophys. J.* **511**, L115-L119 (1999)
- <sup>3</sup>Bernard-Salas, J. *et al.* On the excitation and formation of circumstellar fullerenes. *Astrophys. J.* **757**, 41 (2012)
- <sup>4</sup>Candian, A. *et al.* Searching for stable fullerenes in space with computational chemistry. *Mon. Not. R. Astron. Soc.* **485**, 1137-1146 (2019)